Anti-Cancer Drugs 1998, 9, pp. 58-66

Research paper

Cytotoxicity and intracellular biotransformation of *N*-benzyladriamycin-14-valerate (AD 198) are modulated by changes in 14-*O*-acyl chain length

Leonard Lothstein, Patrick J Rodrigues, Trevor W Sweatman and Mervyn Israel
Department of Pharmacology, University of Tennessee Heath Science Center, 874 Union Avenue, Memphis, TN 38163, USA. Tel: (+1) 901 448-6156; Fax: (+1) 901 448-7300.

_N_-benzyladriamycin-14-valerate (AD 198) is pharmacologically superior to Adriamycin (ADR) based upon comparable cytotoxicity, decreased cardiotoxicity and the ability of AD 198 to circumvent multidrug resistance conferred by either P-glycoprotein overexpression or reduced topoisomerase II activity. AD 198, however, suffers from systemic lability of the 14-*O*-valerate moiety to enzymatic and non-enzymatic cleavage to yield _N_-benzyladriamycin (AD 288), which is more similar to ADR in activity. The purpose of this study was to determine whether stability of the ester linkage could be achieved while preserving the favorable characteristics of AD 198 by using a series of _N_-benzylated ADR congeners containing 14-*O*-acyl substitutions of incrementally shorter carbon chain lengths. Results from this study indicate that the linear five-carbon valerate substitution is the minimum length necessary to circumvent P-glycoprotein and prevent inhibition of topoisomerase II activity. In addition, although AD 198 is not a pro-drug of AD 288, intracellular 14-*O*-acyl cleavage appears to contribute to the cytotoxicity of AD 198.

Key words: Anthracyclines, AD 198, drug resistance, doxorubicin, topoisomerase II.

Introduction

The semisynthetic Adriamycin (ADR) congener *N*-benzyladriamycin-14-valerate (AD 198) has demonstrated improved experimental efficacy over ADR through the circumvention of multidrug resistance conferred by P-glycoprotein (P-gp) overexpression (MDR) or reduced topoisomerase II (topo II) activity (at-MDR) *in vitro* and *in vivo*, and through the absence of cardiotoxicity *in vivo*.[1,2] The efficacy of AD 198, however, may be limited by two factors. First, previous studies have shown that exposure of murine J774.2 macrophage-like cells and P388 lymphocytic leukemia cells to cytotoxic levels of AD 198 could result in the selection of AD 198-resistant (AD 198/R) variants.[3,4] AD 198/R cells displayed a unique resistance phenotype. Despite the overexpression of functional P-gp, intracellular accumulation of AD 198 in AD 198/R cells remains unchanged relative to drug-sensitive cells.[3,4] In addition, changes in the expression and/or activities of topo II, antioxidant enzymes, glutathione-related enzymes and the multidrug-resistance-associated protein (MRP) were not observed.[4] Previous structure-activity studies have compared the intracellular accumulation, subcellular distribution and cytotoxicity of AD 198 in drug-sensitive and AD 198/R J774.2 cells relative to the half-substituted congeners N-benzyladriamycin (AD 288) and adriamycin-14-valerate (AD 48).[5] In contrast to AD 198, AD 288 and AD 48 exhibited reduced intracellular accumulation in AD 198/R cells, suggesting that the addition of either the *N*-benzyl or the 14-valerate moiety was of itself insufficient to prevent transport by P-gp. AD 288 also inhibited topo II-mediated DNA unknotting activity in crude J774.2 nuclear lysates at a 7-fold lower concentration than AD 198. J774.2 cells selected for resistance to AD 288 displayed a typical MDR phenotype.[6] Secondly, AD 288 is the principal metabolite of AD 198 *in vitro* and *in vivo* prior to hepatic metabolism[7] through both enzymatic and non-enzymatic cleavages of the 14-ester linkage. Thus, conversion of AD 198 to AD 288 before target site delivery would potentially limit the efficacy of AD 198, particularly against tumor cells expressing either the MDR or at-MDR phenotypes. In the present study, the length and configuration of the acyl substitution at C-14 of AD 198 was modified to determine whether hydrolytic removal of the 14-*O*-acyl side chain could be suppressed while preserving advantageous cytotoxic properties of AD 198. The results of this study indicate that congeners with 14-*O*-acyl side chains shorter than

Correspondence to L Lothstein

five carbons exhibited cellular characteristics more comparable to AD 288 without stabilization of the 14-ester linkage.

Experimental procedures

Test compounds

AD 198 and AD 288 were prepared as previously described.[8] AD 442, AD 443, AD 444 and AD 445 were prepared for this study according to the following scheme: daunorubicin →14-bromodaunorubicin → 14-*O*-acyladriamycin → 14-*O*-acyl-*N*-benzyladriamycin, where acyl equals acetate, propionate, butyrate and pivalate, respectively. The synthesis of the intermediate 14-*O*-acyladriamycin compounds, where the acyl function is acetate or propionate, was first described by Arcamone *et al.*[9] The corresponding butyrate and pivalate congeners were prepared here in like manner. The 14-*O*-acyladriamycin products thus prepared were converted to their corresponding *N*-benzyl target compounds essentially as described for AD 442, below. Physical and spectral data for the target compounds follow.

Preparation of *N*-benzyladriamycin-14-acetate (AD 442)

Adriamycin-14-acetate (699 mg; 1.195 mmol) and dimethylformamide (15 ml) were placed in a 100 ml round-bottom flask fitted with a ground-glass stopper. With stirring, anhydrous potassium carbonate (187.5 mg) and anhydrous potassium iodide (187.5 mg), both finely powdered, were added and the mixture was stirred for 10 min. Benzyl bromide (150 ml) was then added and the reaction mixture was stirred at room temperature for 2 h, with monitoring by HPLC (conditions below). At the end of the reaction, chloroform (50 ml) and ice-cold water (15 ml) were added and stirring was continued for 5 min, after which time the organic layer was separated and washed with cold water (4 × 15 ml). The combined washings were extracted with chloroform (4 × 15 ml), with the chloroform washes being added to the original organic layer. The combined organic extract was dried overnight over sodium sulfate, then evaporated on the rotovapor leaving a dark red liquid. This was triturated under petroleum ether (50–100 ml aliquots) until it turned into a thick gum. The gummy residue was dissolved in chloroform (10 ml) and the resulting solution poured into petroleum ether (150 ml) to precipitate the product. The crude material was separated by filtration and washed several times with 15 ml portions of petroleum ether; brown powder, 478 mg (59% yield). For purification, the crude product, dissolved in chloroform (15 ml), was loaded onto the top of a silica gel column (30 g) and the column eluted stepwise by gravity flow with chloroform containing increasing amounts of methanol (0, 0.2, 0.3, 0.4, 0.6, 0.8, 1.0, 2.0 and 10%). The bulk of the product eluted with chloroform containing 0.4% methanol; bright orange-colored powder after evaporation of solvent.

Physical characterization of new compounds

All compounds were examined for purity by thin layer chromatography (Analtech glass-backed silica gel plates, 250 μm layer thickness; chloroform: methanol:water, 90:9:1, v/v) and high performance liquid chromatography (4 μm C_{18}-NovaPAK radial compression column; linear gradient from 70%/30% to 10%/90% ammonium formate buffer, 0.05 M, pH 4.0/acetonitrile in 5 min, with final conditions held for 10 min; flow rate 1.0 ml/min; UV, 254 nm, detection). Melting points were determined on a MEL-TEMP laboratory melting point apparatus. Quantitative UV-vis absorption spectra were recorded in methanol on a Perkin-Elmer Lambda 3B spectrophotometer interfaced with a DECstation 325c computer. IR spectra were recorded as KBr pellets on a Mattson FT-IR-2020 Galaxy Series spectrophotometer located in the Department of Chemistry, University of Memphis; all spectral characteristics are consistent with the assigned structures. Nuclear magnetic resonance spectra were kindly recorded by Mr John Miller (Department of Pharmaceutical Sciences, University of Tennessee College of Pharmacy) in $CDCl_3$ on a Bruker ARX300 300 MHz Fourier-transform NMR instrument. Mass spectra were kindly provided by Dr Chhabil Dass, formerly of the University of Tennessee, Memphis, and now located at the University of Memphis. The mass spectra of AD 443, AD 444 and AD 445 were recorded at the University of Tennessee on an AutoSpec Q mass spectrometer as fast atom bombardment (FAB)-positive ion mode spectra and present as M+1 signals; the mass spectrum of AD 442 was recorded at the University of Memphis on a Micromass Platform 2 single quadrapole mass spectrometer under electrospray FAB-negative mode conditions and thus presents as a parent ion (M^+) signal.

N-Benzyladriamycin-14-acetate (AD 442): Melting point 115-12°C. Mass spectrum: *e/z* 675 (M^+). UV-vis absorption spectrum: l_{max} (e) 233 (37450), 251 (25560), 288 (8600), 478 (12200), 495 (12100) and 529 shoulder (6410) nm. Nuclear magnetic resonance spectrum: d 1.42 (3H, doublet, $J=7$ Hz, 5'-CH_3), 2.23 (3H, singlet, $COCH_3$), 4.09 (3H, singlet, 4-OCH_3), 7.28 (5H, singlet, C_6H_5), 7.40 (1H, doublet, $J=8$ Hz, 1-H or 3-H), 7.80 (1H, triplet, $J=8$ Hz, 2-H) and 8.04 (1H, doublet, $J=8$ Hz, 3-H or 1-H) p.p.m.

N-Benzyladriamycin-14-propionate (AD 443): Melting point 135-140°C. Mass spectrum: *e/z* 690 (M+1). UV-vis absorption spectrum: l_{max} (e) 233 (38030), 251 (26120), 288 (8730), 478 (12410), 495 (12280) and 529 shoulder (6470) nm. Nuclear magnetic resonance spectrum: d 1.24 (3H, triplet, $J=7$ Hz, CH_2CH_3), 1.42 (3H, doublet, $J=7$ Hz, 5'-CH_3), 2.52 (2H, doublet, CH_2CH_3), 4.09 (3H, singlet, 4-OCH_3), 7.28 (5H, singlet, C_6H_5), 7.40 (1H, doublet, $J=7$ Hz, 1-H or 3-H), 7.80 (1H, triplet, $J=8$ Hz, 2-H) and 8.05 (1H, doublet, $J=7$ Hz, 3-H or 1-H) p.p.m.

N-Benzyladriamycin-14-butyrate (AD 444): Melting point 200-205°C. Mass spectrum: *e/z* 704 (M+1). UV-vis absorption spectrum: l_{max} (e) 233 (39120), 251 (26740), 288 (8910), 478 (12750), 495 (12610) and 529 shoulder (6670) nm. Nuclear magnetic resonance spectrum: d 1.04 (3H, triplet, $J=7$ Hz, $CH_2CH_2CH_3$), 1.42 (3H, doublet, $J=7$ Hz, 5'-CH_3), 4.10 (3H, singlet, 4-OCH_33), 7.28 (5H, singlet, C_6H_5), 7.40 (1H, doublet, $J=8$ Hz, 1-H or 3-H), 7.80 (1H, triplet, $J=8$ Hz, 2-H) and 8.05 (1H, doublet, $J=8$ Hz, 3-H or 1-H) p.p.m.

N-Benzyladriamycin-14-pivalate (AD 445): Melting point 210-215°C. Mass spectrum: *e/z* 718 (M+1). UV-vis absorption spectrum: l_{max} (e) 233 (38290), 251 (26280), 288 (8720), 478 (12500), 495 (12460) and 529 shoulder (6630) nm. Nuclear magnetic resonance spectrum: d 1.32 (9H, singlet, $C(CH_3)_3$), 1.43 (3H, doublet, $J=7$ Hz, 5'-CH_3), 4.10 (3H, singlet, 4-OCH_3), 7.28 (5H, singlet, C_6H_5), 7.40 (1H, doublet, $J=8$ Hz, 1-H or 3-H), 7.79 (1H, triplet, $J=8$ Hz, 2-H) and 8.05 (1H, doublet, $J=8$ Hz, 3-H or 1-H) p.p.m.

Cell culture

J774.2 mouse macrophage-like parental and AD 198/R cells were maintained in Dulbecco's modified Eagle medium supplemented with 20% donor horse serum as described previously.[3] The AD 198/R variant A300 was selected and continuously maintained on 300 nM AD 198. Media and drug were replenished at 48-72 h intervals.

Drug cytotoxicity analysis

IC_{50} values (drug concentration that inhibited cell proliferation by 50%) were determined by the MTT assay.[10] J774.2 and A300 cells were seeded in 96-well microtiter plates at an initial density of 2.5×10^4 cells/ml and, before addition of MTT and solubilization buffer, exposed to drug either continuously for 72 h, or for 1 h followed by incubation for 71 h in drug-free medium. Values represent the mean of at least three independent determinations performed in triplicate.

Intracellular drug metabolism

J774.2 and A300 cells were suspended in pre-warmed culture medium at a density of 1×10^6/ml and incubated in 1 μM drug at 37°C at 7.5% CO_2 with periodic agitation. At the times indicated, 1 ml aliquots were removed, pelleted and washed in cold PBS. Drug was extracted from the cell pellets and medium, and quantified by fluorescence HPLC as previously described.[11]

Intracellular drug accumulation

J774.2 and A300 cells were treated with drug as described for drug metabolism studies. Cells were then pelleted, washed in PBS and resuspended in fresh PBS. Fluorescence content was quantified by flow cytometry with a Coulter Profile 11 instrument utilizing 15 mW of 488 argon ion laser light excitation. Fluorescence emission analysis was performed through a 590 nm long pass filter on a cell population defined by forward angle light scatter and side angle light scatter. Mean log fluorescence (arbitrary units) represents three independent determinations.

Confocal laser scanning microscopy

J774.2 and A300 cells were exposed to 1.0 M drug for 1 h in multiwell chamber slides under conditions described previously.[3,5] Samples were observed by chromophore excitation at 568 nm using a BioRad 1000 confocal laser scanning microscope equipped with a krypton/argon ion laser. Images represent 1000× magnification.

Topo II decatenation activity assay

Nuclear extracts of J774.2 cells were prepared in 0.35 M NaCl as described[12] with the addition of a

protease inhibitor cocktail.[4] The nuclear extract protein content was determined by a colorimetric assay (BioRad, Richmond CA) based upon the procedure of Bradford.[13] Decatenation activity was measured using catenated networks of double-stranded kinetoplast DNA (kDNA) circles as a substrate.[14] Briefly, 75 ng of nuclear lysate protein, 75 ng of catenated kDNA and drug dissolved in DMSO were combined in reaction buffer (50 mM Tris-HCl, pH 7.5, 100 mM KCl, 10 mM $MgCl_2$, 0.5 mM DTT, 0.5 mM EDTA, 30 μg/ml BSA and 0.25 mM ATP) and incubated at 37°C for 90 min. The reaction was terminated with 0.5% SDS (v/v) and 150 μg/ml proteinase K for 1 h at 37°C. Topological forms of kDNA were resolved by 1% agarose gel electrophoresis in Tris-borate/EDTA buffer with 0.5 μg/ml ethidium bromide. DMSO concentrations in each reaction were maintained at 0.8% by addition of equal volumes of serially diluted drug stocks.

Results

The anthracycline congener series AD 198, AD 445, AD 444, AD 443 and AD 442 have attached to the C-14 position, via an ester linkage, acyl side chains of decreasing length (Figure 1). The carbon chain length has been either progressively foreshortened at one-carbon increments (AD 198, AD 444, AD 443 and AD 442) or rearranged to form a trimethyl tertiary carbon (AD 445) isomeric with AD 198.

Foreshortening the 14-O-acyl chain length had little effect in altering the rate of intracellular hydrolysis of the ester linkage of the substitutions (Figure 2). AD 442, AD 443 and AD 444 exhibited identical rates of deacylation in the initial 5 h of uptake into J774.2 cells compared to AD 198, with approximately 40% conversion of parent compound to AD 288. Hydrolysis of the 14-O-acyl side chains in AD 444 and AD 443 continued at a rate similar to AD 198 after 16 h of intracellular incubation. AD 442, however, was 97% hydrolyzed to AD 288. In contrast, AD 445 exhibited an initial 15% hydrolysis within 1 h of uptake into J774.2 cells, but without further bioconversion during the subsequent 15 h of exposure. Since the 14-O-acyl congeners exhibited rapid rates of conversion to AD 288, drug cytotoxicity was determined following the treatment of drug-sensitive (J774.2) and AD 198-resistant J774.2 cells (A300) for 1 h in addition to a 72 h continuous drug exposure, which would measure combined cytotoxicity of parent drug and biotransformation product (Table 1). Cytotoxicity of AD 442, AD 443 and AD 444 in J774.2 cells was similar to AD 198 after 1 h exposure, and marginally less than

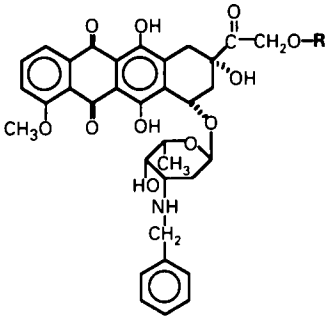

Name	Code No.	R
N-Benzyladriamycin	AD 288	H
N-Benzyladriamycin-14-acetate	AD 442	$\overset{O}{\overset{\|}{C}}CH_3$
N-Benzyladriamycin-14-propionate	AD 443	$\overset{O}{\overset{\|}{C}}CH_2CH_3$
N-Benzyladriamycin-14-butyrate	AD 444	$\overset{O}{\overset{\|}{C}}CH_2CH_2CH_3$
N-Benzyladriamycin-14-pivalate	AD 445	$\overset{O}{\overset{\|}{C}}-\overset{CH_3}{\overset{\|}{C}}-CH_3$ (CH₃)
N-Benzyladriamycin-14-valerate	AD 198	$\overset{O}{\overset{\|}{C}}CH_2CH_2CH_2CH_3$

Figure 1. Chemical structures of 14-O-acyl *N*-benzyladriamycin congeners.

both AD 288 and AD 198 after 72 h exposure. AD 445 was 2- and 5-fold less cytotoxic than AD 198 in J774.2 cells after 1 and 72 h exposures, respectively. Selection of A300 cells in 300 nM AD 198 resulted in 15.3-fold resistance to AD 198 following 72 h of continuous drug exposure and 2.3-fold following 1 h exposure. Likewise, similar patterns of cross-resistance were observed for each of the acyl chain substitutions and for AD 288, with AD 442 exhibiting the lowest level of cross-resistance following 1 and 72 h exposures.

Resistance to AD 198 did not coincide with a significant decrease in intracellular AD 198 accumulation despite the overexpression of P-gp in A300 cells.[5] AD 288, which was shown to be a substrate for P-gp, exhibited reduced accumulation in MDR cells.[5] Therefore, net intracellular levels of AD 442, AD 443, AD 444 and AD 445 were measured by fluorescence HPLC to assess the effect of 14-O-acyl chain length on accumulation in drug-sensitive cells and presumptive transport by P-gp in MDR cells (Figure 3). Net intracellular accumulation in J774.2 cells of the 14-O-acyl congeners exhibited a mean 45% increase over AD 288, probably owing to the

increased lipophilicity conferred by acyl chain substitution at C-14.[15] No significant difference in accumulation in J774.2 cells was observed between the AD 198 and any of the congeners. In A300 cells, accumulation of AD 288 was reduced 80%, due to transport by P-gp. Accumulation of AD 442, AD 443, AD 444 and AD 445 were all reduced 55%. However, accumulation of AD 198 exhibited only a 20% decrease under these conditions.

Addition of the valerate moiety at C-14 with or without *N*-benzylation at C-3′ resulted in cytoplasmic localization of ADR congeners.[5] Therefore J774.2 cells were exposed to the 14-*O*-acyl congeners to determine the effect of incremental changes in 14-*O*-acyl chain length on subcellular drug distribution (Figure 4). AD 288 accumulated rapidly within the nucleus of both J774.2 and A300 cells, with little detectable cytoplasmic fluorescence. AD 288 localization in the nucleus was characterized by intense, granular fluorescence, indicative of AD 288 association with interphase chromatin. Metaphase chromosomes could be identified by AD 288 fluorescence (not shown). J774.2 cells that were treated with AD 442, AD 443 and AD 444 exhibited predominantly nuclear fluorescence similar to AD 288, but also diffuse cytoplasmic fluorescence that became more prominent with increasing alkylester chain length. AD 445 exhibited significant cytoplasmic localization in both cell lines, yet with nuclear fluorescence still evident. AD 198 was localized primarily in the perinuclear cytoplasm of J774.2 and A300 cells. Although some nuclear fluorescence was apparent, the pattern differed markedly from AD 288 and may reflect cytoplasmic fluorescence surrounding the nucleus. An identical pattern of subcellular drug distribution was observed in A300 cells (not shown). These results indicate that increasing acyl chain length at C-14 progressively altered subcellular distribution of anthracyclines in favor of cytoplasmic localization.

Previous studies have shown that AD 198 was much less effective in inhibiting topo II-mediated

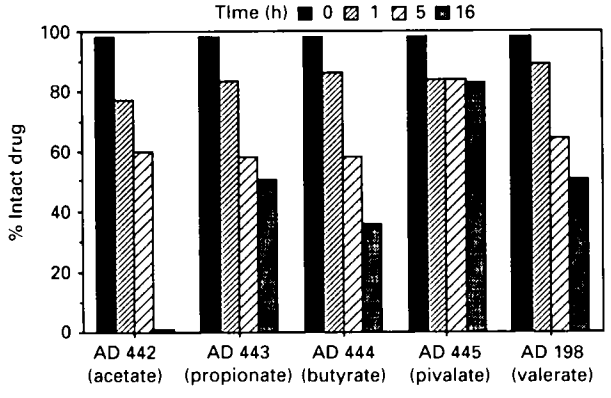

Figure 2. Intracellular anthracycline metabolism. J774.2 and A300 cells at 1×10^6 cells/ml were treated with 1 μM drug at 37 C for the time periods indicated. Intracellular drug was extracted and analyzed by fluorescence HPLC. Drug metabolism is represented by the percentage of intact drug remaining within the cell.

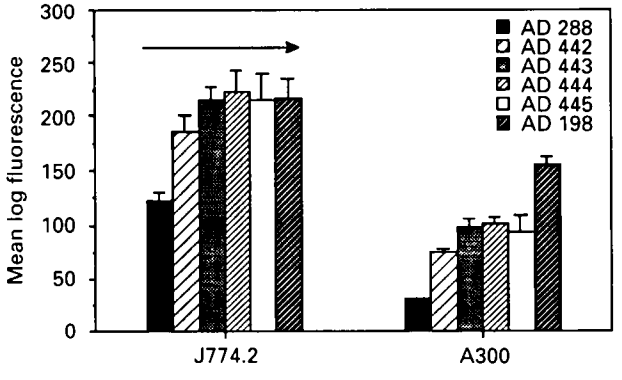

Figure 3. Net intracellular anthracycline accumulation. J774.2 and A300 cells at 1×10^6 cells/ml were treated with 1 μM drug for 1 h at 37 C. Flourescence emissions of cells were quantified by flow cytometry ($\lambda_{excitation} - 488$ nm, $\lambda_{emission} - > 590$ nm). Mean log fluorescence (arbitrary units) represents three independent determinations.

Table 1. Cytotoxicity analyses of 14-*O*-Acyl *N*-benxyladriamycin congeners [IC_{50}[a] ± SE (*n*-fold resistance)]

	1 h (μM IC_{50})		72 h (nM IC_{50})	
	J774.2	A300	J774.2	A300
AD288	4.3±0.2 (1)	7.4±0.4 (1.7)	45.0±8.0 (1)	543.0±77.0 (12.1)
AD442	7.6±0.6 (1)	8.9±0.4 (1.2)	27.7±3.2 (1)	192.4±34.3 (7.0)
AD443	10.2±2.1 (1)	24.2±2.3 (2.4)	26.2±6.9 (1)	455.9±106.9 (17.4)
AD444	10.5±1.3 (1)	16.0±3.5 (1.8)	38.1±1.8 (1)	421.0±59.0 (11.1)
AD445	26.7±2.4 (1)	66.1±4.3 (2.5)	262.4±25.4 (1)	1885.0±165.0 (7.2)
AD198	11.5±1.5 (1)	26.2±0.4 (2.3)	49.0±2.3 (1)	750.0±78.0 (3.0)

[a] Drug concentration that inhibited cell proliferation by 50% after indicated exposure time, as determined by the MTT assay.

DNA cleavage, compared with ADR and AD 288.[4,16] Thus, the ability of the 14-*O*-acyl congeners to inhibit topo II activity within the crude nuclear lysates of J774.2 cells was compared with changes in 14-*O*-acyl chain length. Activity of topo II was monitored by the decatenation of linked, circular kDNA from *C. fasciculata* (Figure 5). Due to its size, catenated kDNA cannot migrate into 1% agarose and remained within the well. In the absence of drug, 75 ng of crude nuclear lysate contained sufficient topo II activity to completely decatenate 100 ng of kDNA into individual circular forms, thus permitting electrophoretic migration (lane 0). Increasing concentrations of AD 288 in the reaction mixture caused progressive inhibition of topo II decatenation activity, with complete inhibition occurring in 1 μM AD 288. AD 442 and AD 443 were slightly less effective, with complete inhibition at 2 μM. AD 444 was still less effective (3 μM), while AD 445 (7 μM) and AD 198 (12 μM) were significantly less effective at inhibiting topo II. Low levels of monomer kDNA were observed in 16 μM AD 198. These results indicate that substitution at C-14 with an acyl moiety of increasing carbon chain length decreased the topo II inhibitory potency of the anthracycline, with a marked decreased occurring with the valerate substitution.

Discussion

The current approach to the design of more effective antitumor anthracyclines is through modification of structural components associated with specific cellular or systemic effects.[17-19] Typical of this approach is AD 198, in which specific structural changes have resulted in several clinically advantageous characteristics. These include increased lipophilicity leading to more rapid tumor penetration and membrane-active properties, reduced cardiotoxicity, reduced hematotoxicity, and circumvention of P-gp- and topo II-mediated multidrug resistance in cultured tumor cells.[1,2] Circumvention of multidrug resistance by AD 198 was achieved only by the combined 3′-*N*-benzyl and 14-valerate substitutions, since (i) AD 288 was both a substrate for P-gp[5] and a potent inhibitor of topo II[4] (Figure 5), and (ii) adriamycin-14-valerate was a substrate for P-gp-mediated transport.[5] Therefore, protection of the 14-*O*-ester linkage from hydrolysis prior to target site delivery would be advantageous in preserving the unique cytotoxic profile of AD 198. To some extent, this has been achieved. As has been shown in rats 15 min after injection of AD 198 into the tail vein, AD 288 levels relative to AD 198 reached 10-15% in lung, heart and brain, while reaching 35-45% in liver, kidney and gut.[20] Since conversion of AD 198 to

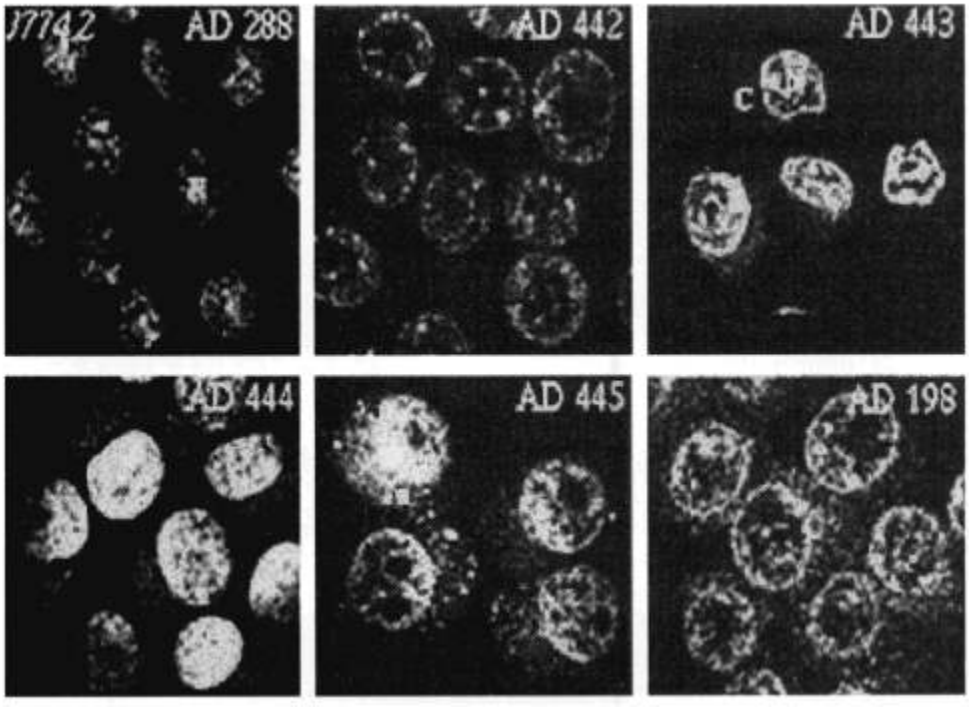

Figure 4. Subcellular anthracycline distribution. Monolayer J774.2 and A300 cells were treated with 1 μM of the indicated drug for 1 h at 37°C, washed with PBS and observed by confocal laser scanning microscopy. Excitation of the anthracycline chromophores at 568 nm was achieved with a krypton/argon ion laser. N, nucleus, C, cytoplasm. Magnification 1000×.

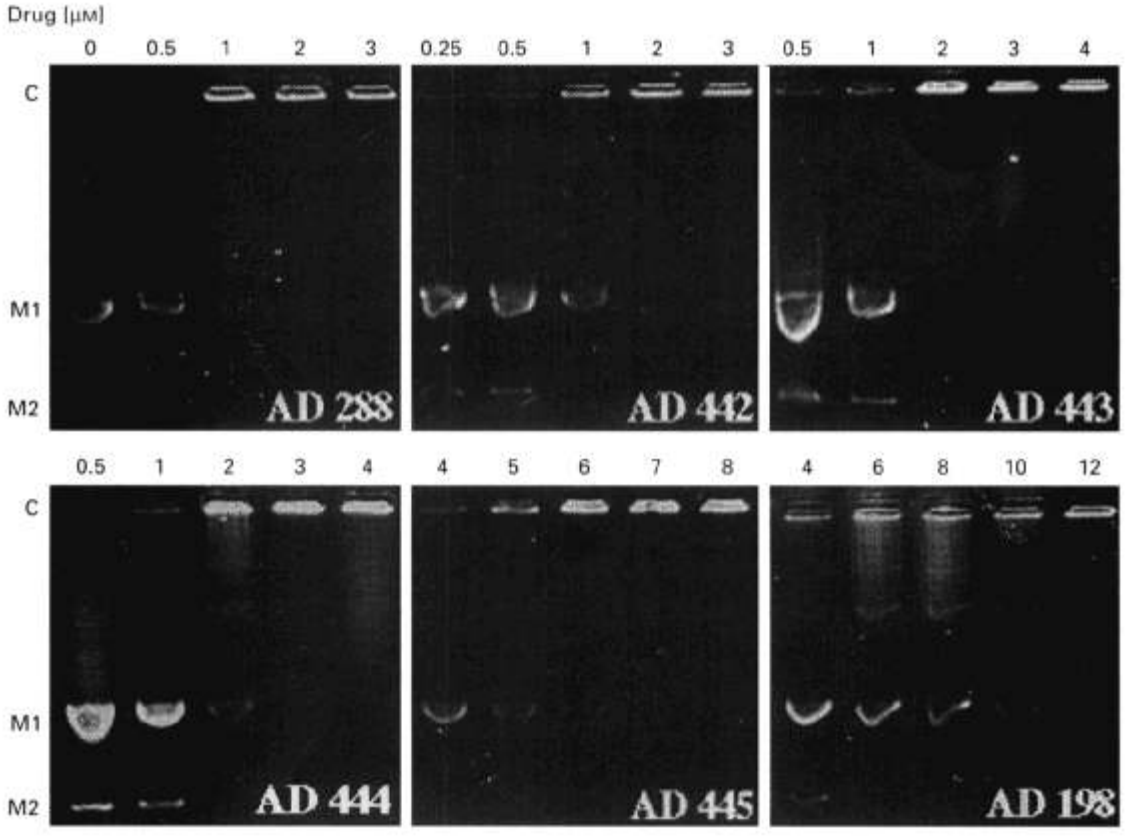

Figure 5. Topo II inhibition by 14-*O*-acyl congeners of AD 198. Nuclear lysate (75 ng) from J774.2 cells was incubated for 90 min with 125 ng catenated kDNA and either DMSO alone (lane 0) or increasing pM concentrations of drug, as indicated in each panel. Treated kDNA was resolved by electrophoresis in 1.0% agarose in Tris–borate/EDTA buffer with ethidium bromide. Catenated kDNA (C) did not migrate into the gel. M1 and M2 indicate the position of nicked and relaxed kDNA species, respectively.

AD 288 in lung was slow,[20] much of the AD 288 found in the lung 15 min post-injection was probably due to biotransformation before entry into lung tissue. Thus, conversion of AD 198 to AD 288 probably increased with time between injection and tissue adsorption. Inhibition of ester hydrolysis would increase the amount of AD 198 delivery to target site and persistence of intact drug within the target cells. Consequently, the goal of this study was to determine whether 14-*O*-acyl chain length could be modified in such a way as to inhibit ester hydrolysis while retaining the therapeutically beneficial characteristics of AD 198. It had been determined previously that lengthening the carbon chain of the 14-*O*-acyl moiety did not significantly affect the ester cleavage rate.[21] In addition, substitution of the oxy-ester linkage with a thioester in *N*-(trifluoroacetyl)adriamycin-14-valerate (AD 32) doubled the $T_{1/2}$ of ester hydrolysis, but increased the IC_{50} value by greater than 20-fold.[22] Replacement of the oxy-ester bridge with a more stable thioether bridge in AD 32 increased the IC_{50} value 23-fold.[23] In AD 32, 14-*S*-acyl chain length modification resulted in changes in both thioester linkage stability and cytotoxicity. Optimal stability was observed with the 14-*S*-propionate congener with a $T_{1/2}$ of ester hydrolysis 8-fold greater than AD 32. The 14-*S*-propionate congener also exhibited the highest cytotoxicity of the 14-*S*-ester series, albeit with an IC_{50} value still 10-fold greater than AD 32. The present study demonstrated that shortening the 14-*O*-acyl chain length in AD 198 by one-carbon increments did not significantly change either the stability of the ester linkage or the cytotoxicity of the congener in either drug-sensitive or AD 198-resistance J774.2 cells. Reconfiguration of the valerate side-chain to form a trimethylester caused marked stabilization of the 14-*O*-ester linkage, presumably through steric protection of the ester bonds, with an accompanying 2.4-fold decrease in cytotoxicity based upon 1 h drug exposure cytotoxicity assays. Therefore, it appears that stabilization of the 14-*O*-ester bridge reduced anthracycline cytotoxicity.

The structural determinants for substrate recognition by P-gp remain broad and controversial. However, lipophilic compounds with one or more planar aromatic rings and a basic site are often substrates for P-gp.[24-27] AD 198, in theory, satisfies these requirements and in addition inhibits azidopine binding to P-gp in isolated membrane fragments from MDR J774.2 cells.[4,28] Nevertheless, AD 198 remains highly cytotoxic against MDR cell lines,[1,29] owing at least in part to intracellular retention of AD 198 in MDR cells at levels similar to drug-sensitive cells. AD 198 avoided transport by P-gp through reduced substrate recognition and rapid subcellular sequestration, due, in part, to the lipophilicity of AD 198 despite the preservation of positive charge.[3,4,30] The membrane-disruptive effects of AD 198 may also lead to allosteric inhibition of P-gp function,[4] much in the same manner that the detergents Cremophor EL and Tween 80 have on P-gp photolabeling.[28] AD 288 lacks the membrane effects of AD 198[2] and demonstrated a marked decrease in affinity for unilamellar phospholipid membranes compared with AD 198.[15] The lipophilicity of the 14-*O*-acyl congeners described here is likely to span the difference between AD 288 and AD 198, and may represent a critical range in determining cytotoxicity in MDR cells. Consequently, the intermediate levels of intracellular 14-*O*-acyl congeners in A300 cells may have been the result of less extensive membrane disruption and consequent decreased P-gp inhibition.

Circumvention of at-MDR by AD 198 has been attributed to the inability of AD 198 to stimulate formation of the topo II-DNA cleavable complex and generate DNA cleavage fragments.[4,16] This, in turn, is attributed to the inhibition of drug-topo II interaction by the 14-*O*-valerate substitution.[16] The extent of inhibition appears to correlate with 14-*O*-acyl chain length, as demonstrated in the kDNA decatenation assays described in Figure 4. As the 14-*O*-acyl moiety was elongated, the concentration of drug required to inhibit decatenation increased, suggesting a progressive steric inhibition of drug-topo II interaction. This would be predicted based upon the delineation of anthracycline functional domains with respect to DNA and topo II interaction.[31] In this scheme, the enzyme interacting domain tends to encompass the chromophore A ring and its additions. Consistent with this model and our results are studies by Jensen *et al.*[32] demonstrating that substitution of a carboxymethyl group in place of the hydroxyl at C-10 of the aglycone 6-rhodomycinone inhibited drug-induced cleavable complex formation. Thus, introduction of bulkier substituents on several A ring sites of the chromophore interferes with topo II-drug interaction. Drug-topo II interaction can be mediated by substitutions at other sites on the anthracycline, such as C-4[31] and C-3'.[16,32,33] The effects of substitutions at C-3' on cleavable complex formation are less predictable than on the A ring. The presence of a bulky benzyl group, as in AD 288, has little effect on drug action, while 3'-*N*-dimethylation abolishes DNA cleavage.[16,32] Hydroxylation at C-3' maintains potent stimulation of DNA cleavage and permits selection of the at-MDR phenotype.[34,35]

These results further elucidate several aspects of anthracycline drug design and circumvention of multidrug resistance. First, the five-carbon valerate configuration appears to be the minimum length required to significantly circumvent P-gp-mediated transport. Second, the five-carbon substitution is the minimum length required to substantially block drug-mediated topo II inhibition. While the ability of AD 198 to circumvent at-MDR has been established,[1] the cytotoxicity of AD 442, AD 443, AD 444 or AD 445 relative to ADR or AD 198 in an at-MDR cell line is being tested. Third, inhibition of 14-ester cleavage reduces drug cytotoxicity, suggesting that the cytotoxicity of 14-*O*-acyl substituted congeners is due in part to the presence of metabolite. Fourth, the reduced inhibition of topo II by AD 198, compared to AD 288, and the ability of AD 198 to effectively circumvent at-MDR further indicates that AD 198 is not merely a pro-drug of AD 288. Rather, AD 198 operates through a cytotoxic mechanism distinct from that of AD 288. This novel mechanism is currently under investigation. Increased cytotoxicity produced by 14-*O*-ester cleavage may result from either the additive effect of AD 288 cytotoxicity following redistribution into the nucleus[5] or AD 288 cytotoxicity at the same cytoplasmic target sites as AD 198.

Acknowledgments

The authors are indebted to Ms Luydmilla Savranskaya for excellent technical assistance. This work was supported in part by American Cancer Society Research Investigation grant BE-137 (LL), Milheim Foundation for Cancer Research grant 94-35 (LL), NIH grant CA 44890 (TWS) and by The Anthra Pharmaceuticals Research Fund (MI).

References

1. Sweatman TW, Israel M, Koseki Y, *et al.* Cytotoxicity and cellular pharmacology of *N*-benzyladriamycin-14-valerate in mechanistically different multidrug-resistant human leukemic cells. *J Cell Pharmacol* 1990; **1:** 95-102.
2. Israel M, Seshadri R, Koseki, Y, *et al.* Amelioration of adriamycin toxicity through modification of drug-DNA binding properties. *Cancer Treat Rev* 1987; **14:** 163-7.

3. Lothstein L, Sweatman TW, Dockter ME, *et al.* Resistance to *N*-benzyladriamycin-14-valerate in mouse J774.2 cells: P-glycoprotein expression without reduced *N*-benzyladriamycin-14-valerate accumulation. *Cancer Res* 1992; **52:** 3409–17.
4. Lothstein L, Koseki Y, Sweatman TW. P-glycoprotein overexpression in mouse cells does not correlate with resistance to *N*-benzyladriamycin-14-valerate (AD 198). *Anti-Cancer Drugs* 1994; **5:** 623–33.
5. Lothstein L, Wright H, Sweatman TW, *et al. N*-Benzyladriamycin-14-valerate and drug resistance: correlation of anthracycline structural modifications with intracellular accumulation and distribution in multidrug resistant cells. *Oncology Res* 1992; **4:** 341–34.
6. Lothstein L, Sweatman W, Dockter ME, *et al.* Differential distribution of *N*-benzyladriamycin-14-valerate (AD 198) and *N*-benzyladriamycin (AD 288) in multidrug-resistant mouse J774.2 cells. *Proc Am Ass Cancer Res* 1991; **32: 356.**
7. Sweatman TW, Seshadri R, Israel M. Metabolism and elimination of *N*-benzyladriamycin-14-valerate (AD 198) in the rat. *Proc Am Ass Cancer Res* 1989; **30:** 532.
8. Israel M Seshadri R. US Patent no. 4,610,977, 1989.
9. Arcamone F, Franceschi G, Minghetti A, *et al.* Synthesis and biological evaluation of some 14-*O*-acyl derivatives of adriamycin. *J Med Chem* 1974; **17:** 335–7.
10. Mossman T. Rapid colorimetric assay for cellular growth and survival: application to proliferation and cytotoxicity assays. *J Immunol Methods* 1983; **65:** 55–63.
11. Israel M, Sweatman TW, Seshadri R, *et al.* Comparative uptake and retention of Adriamycin and *N*-benzyladriamycin-14-valerate in human CEM leukemic lymphocyte cell cultures. *Cancer Chemother Pharmacol* 1989; **25:** 177–83.
12. Danks MK, Schmidt CA, Cirtain MC, *et al.* Altered catalytic activity of and DNA cleavage by DNA topoisomerase II from human leukemic cells selected for resistance to VM-26. *Biochemistry* 1988; **27:** 8861–9.
13. Bradford M. A rapid and sensitive method for the quantitation of microgram quantities of protein utilizing the principle of protein-dye binding. *Anal Biochem* 1976; **72:** 248–54.
14. Sahai BM, Kaplan GK. A quantitative decatenation assay for type II topoisomerases. *Anal Biochem* 1986; **156:** 364–79.
15. Burke TG, Israel M, Seshadri R, *et al.* A fluorescence study examining how 14-valerate side chain substitution modulates anthracycline binding to small unilamellar phospholipid vesicles. *Biochim Biophys Acta* 1989; **982:** 123–30.
16. Bodley A, Liu LF, Israel M, *et al.* DNA topoisomerase II-mediated interaction of doxorubicin and daunorubicin congeners with DNA. *Cancer Res* 1989; **49:** 5969–78.
17. Israel M, Seshadri R, Koseki Y, *et al.* Amelioration of adriamycin toxicity through modification of drug–DNA binding properties. *Cancer Treat Rev* 1987; **14:** 163–7.
18. Priebe W, Perez-Soler R. Design and tumor targeting of anthracyclines able to overcome multidrug resistance: a double-advantage approach. *Pharmacol Ther* 1993; **60:** 215–34.
19. Priebe W. Mechanism of action-governed design of anthracycline antibiotics: a turn-off/turn-on approach. *Current Drug Design* 1995; **1:** 73–96.
20. Sweatman TW, Seshadri R, Israel M. Selective retention of *N*-Benzyladriamycin-14-valerate (AD 198) in the rat lung following intravenous drug administration. *Proc Am Ass Cancer Res* 1992; **33:** 520.
21. Lothstein L, Hosey LM, Sweatman TW, *et al. N*-benzyladriamycin-14-valerate-resistant cells exhibit cross-resistance to other anthracycline analogs that circumvent multidrug resistance. *Oncol Res.* 1993; **5:** 229–34.
22. Seshadri R, Idriss JM, Israel M. Adriamycin analogues. Preparation and biological evaluation of some thio ester analogues of adriamycin and *N*-(trifluoroacetyl)adriamycin-14-valerate. *J Med Chem* 1986; **129:** 1269–73.
23. Seshadri R, Israel M, Pegg WJ. Adriamycin analogues. Preparation and biological evaluation of some novel 14-thioadriamycins. *J Med Chem* 1983; **26:** 11–5.
24. Lampidis TJ, Castello C, Del Giglio A, *et al.* Relevance of the chemical charge of rhodamine dyes to multiple drug resistance. *Biochem Pharmacol* 1989; **38:** 4267–71.
25. Tang-Wai DF, Brossi A, Arnold LD, *et al.* The nitrogen of the acetamido group of colchicine modulates P-glycoprotein-mediated multidrug resistance. *Biochemistry* 1993; **32:** 6470–6.
26. Priebe W, Van NT, Burke TG, *et al.* Removal of the basic center from doxorubicin partially overcomes multidrug resistance and decreases cardiotoxicity. *Anti-Cancer Drugs* 1993; **4:** 37–48.
27. Zamora JM, Pearce HL, Beck WT. Physical-chemical properties shared by compounds that modulate multidrug resistance in human leukemic cells. *Mol Pharmacol* 1988, **33:** 454–62.
28. Friche E, Demant EJF, Sehested M, *et al.* Effect of anthracycline analogs on photolabelling of P-glycoprotein by [^{125}I]iodomycin and [^{3}H]azidopine: relation to lipophilicity and inhibition of daunorubicin transport in multidrug resistant cells. *Br J Cancer* 1993; **67:** 226–31.
29. Ganapathi R, Grabowski D, Sweatman TW, *et al. N*-benzyladriamycin-14-valerate versus progressively doxorubicin-resistant murine tumours: cellular pharmacology and characterization of cross-resistance *in vitro* and *in vivo*. *Br J Cancer* 1989; **60:** 819–26.
30. Lampidis TJ, Kolonias D, Podona, T, *et al.* Circumvention of P-gp MDR as a function of anthracycline lipophilicity and charge. *Biochemistry* 1997; **36:** 2679–85.
31. Capranico G, Butelli E, Zunino F. Change of the sequence specificity of daunorubicin-stimulated topoisomerase II DNA cleavage by epimerization of the amino group of the sugar moiety. *Cancer Res* 1995; **55:** 312–7.
32. Jensen PB, Sorensen BS, Sehested M, *et al.* Different modes of anthracycline interaction with topoisomerase II. *Biochem Pharmacol* **45:** 2025–35.
33. Capranico G, Zunino F, Kohn KW, *et al.* Sequence-selective topoisomerase II inhibition by anthracycline derivatives in SV40 DNA: relationship with DNA binding affinity and toxicity. *Biochemistry* 1990; **29:** 562–9.
34. Solary E, Ling Y-H, Perez-Soler R, *et al.* Hydroxyrubicin, a deaminated derivative of doxorubicin, inhibits mammalian DNA topoisomerase II and partially circumvents multidrug resistance. *Int J Cancer* 1994; **58:** 85–94.
35. Lothstein L, Sweatman TW, Priebe W. Hydroxylation at C-3′ of doxorubicin alters the selected phenotype of cellular drug resistance. *Bioorg Med Chem* 1995; **5:** 1807–12.

(Received 9 September 1997; accepted 18 September 1997)